

TEMPERATURE AND HUMIDITY PROFILES IN THE ATMOSPHERE FROM SPACE BORNE LASERS  
( a feasibility study )

Hartmut Grassl and Peter Schlüssel  
Institut für Meereskunde  
Düsternbrooker Weg 20  
D - 2300 Kiel 1 , FRG

ABSTRACT

Computer simulations of the differential absorption lidar technique in a space craft for the purpose of temperature and humidity profiling indicate:

- 1) Current technology applied to O<sub>2</sub> and H<sub>2</sub>O lines in the .7 to .8 μm wavelength band gives sufficiently high signal-to-noise ratios (up to 50 for a single pulse pair) if backscattering by aerosol particles is high, i.e. profiling accurate to 2 K for temperature and 10 % for humidity should be feasible within the turbid lower troposphere in 1 km layers and with an averaging over approximately 100 pulses.
- 2) The impact of short term fluctuations in aerosol particle concentration is too big for a one laser system. Only a two laser system firing at a time lag of about 1 millisecond can surmount these difficulties.
- 3) The finite width of the laser line and the quasi-random shift of this line introduce tolerable, partly systematic errors.

1. INTRODUCTION

The retrieval of temperature and humidity profiles from radiances measured with current space borne passive radiometers mainly suffers from a poor height resolution. Therefore any system increasing the number of independent informations - equivalent to enhanced height resolution - at the same or even slightly reduced accuracy level is highly desirable. The present study simulates the backscattering of laser light by the atmosphere to a space craft flying at 250 or 800 km above the earth surface. The main goals of this study, temperature and humidity profiles, need at least two wavelengths, while the aerosol backscattering profiles in clear atmospheres and above clouds as well as cloud top detection can be determined from a single wavelength lidar.

We report on temperature and humidity profiles from a two wavelength differential absorption lidar (DIAL). Quite a number of parameters, which all influence the backscattering of laser light and the accuracy of its detection have been set to realistic values or varied within realistic ranges in order to assess their impact on the signal-to-noise ratio (SNR):

- tropospheric and stratospheric aerosol particles
- absorber amount (for humidity profiles only)
- laser power (remaining within technologically feasible ranges)
- instability of the laser wavelength
- width of the laser line
- shift of the O<sub>2</sub> or H<sub>2</sub>O line center with atmospheric pressure
- time integration (equivalent to layer thickness desired)
- line shape of the atmospheric absorption line
- space averaging (necessary to increase SNR)

## 2. BASIC EQUATIONS

We start with the lidar equation describing the power received at the detector  $P(r)$  after backscattering of laser power  $P_0$  by a substance at distance  $r$ .

$$P(r) = P_0 \eta_0 \eta_1 A^* \frac{\tau c}{2} \cdot \frac{1}{r^2} \beta(r) \exp\left(-2 \int_0^r e(r') dr'\right) \quad (1)$$

with  $P_0$  = emitted laser power accounting for losses within the laser optics

$\eta_0$  = correction for beam overlapping

$\eta_1$  = optical efficiency of the receiving system

$A^*$  = effective receiver area

$\tau$  = pulse length

$c$  = velocity of light

$\beta(r)$  = backscattering coefficient at distance  $r$

$e(r)$  = extinction coefficient at distance  $r' = r$

Discretization of the integral in (1) into  $m$  finite layers with thickness  $\Delta r$  and formulation for two wavelengths  $\lambda_1$  and  $\lambda_2$  leads to the ratio of signals

$$\frac{P(\tau, \lambda_1)}{P(\tau, \lambda_2)} = \frac{\beta(\tau, \lambda_1)}{\beta(\tau, \lambda_2)} \cdot \frac{\prod_{i=1}^{m=r/\Delta r} \exp(-2e(\tau', \lambda_1)\Delta r)}{\prod_{i=1}^m \exp(-2e(\tau', \lambda_2)\Delta r)} \quad (2)$$

where  $r' = r - \Delta r/2$  has been introduced. Writing (2) in terms of the layer  $i-1$  leads to a recursion formula, which - after the neglect of the wavelength dependence of  $\beta$  (certainly valid for  $\Delta\lambda \leq 2\text{nm}$ ) - is reduced to

$$\frac{P(\tau, \lambda_1)}{P(\tau, \lambda_2)} = \frac{P(\tau - \Delta r, \lambda_1)}{P(\tau - \Delta r, \lambda_2)} \cdot \frac{\exp(-2k(\tau', \lambda_1)\Delta r)}{\exp(-2k(\tau', \lambda_2)\Delta r)}$$

Resolved for the differential absorption coefficient  $\Delta k(r') = k(r', \lambda_1) - k(r', \lambda_2)$  we get

$$\Delta k(r') = -\frac{1}{2\Delta r} \cdot \ln \left( \frac{P(\tau, \lambda_1) \cdot P(\tau - \Delta r, \lambda_2)}{P(\tau, \lambda_2) \cdot P(\tau - \Delta r, \lambda_1)} \right) \quad (3)$$

If one laser wavelength,  $\lambda_2$ , is in a window between absorption lines, the differential absorption coefficient  $\Delta k(r') = k(r', \lambda_1)$ . Now adopting the Lorentz line shape the absorption coefficient at wavenumber  $\nu$  reads

$$k_\nu(r') = \frac{S(r')}{\pi} \cdot \frac{\alpha(r')}{(\nu - (\nu_0 - \gamma(r')))^2 + \alpha(r')^2} \quad (4)$$

where  $S$  = line intensity depending on temperature  $T$

$\nu_0$  = central wavenumber at standard conditions

$\alpha$  = line halfwidth depending on  $T$  and pressure  $p$

$\gamma$  = line shift depending on  $T$  and  $p$

we introduce one of the desired parameters: temperature  $T$ .

Accounting for the temperature and pressure dependence of  $S$  and

$$S(r') = S_0 n(r') \left( \frac{T_0}{T(r')} \right)^\delta \exp \left( - \frac{E_0}{k_0} \left( \frac{1}{T(r')} - \frac{1}{T_0} \right) \right)$$

$$\alpha(r') = \alpha_0 \cdot \frac{p(r')}{p_0} \cdot \left( \frac{T_0}{T(r')} \right)^{1/2} \quad (5)$$

we have to handle some more parameters,

- $S_0$  = line strength at reference temperature  $T_0$
- $E_0$  = energy of the lower state
- $k_0$  = Boltzmann's constant
- $\delta$  = molecular constant depending on degrees of freedom for rotation  
( $\delta = 1$  for linear molecules,  $\delta = 1.5$  for  $H_2O$ )
- $\alpha_0$  = halfwidth at  $T_0, p_0$
- $p_0$  = 1 atm pressure

but we also find the second desired parameter: the number density  $n(r')$  of the molecule having a line at  $\nu_0$ . Insertion of (4) for  $\nu = \nu_0$  and of (5) into (3) gives the basic equation for temperature determination as long as  $n/p$  is known.

$$k_\nu = \frac{S_0 p_0}{1.132 \pi \alpha_0} \cdot \frac{n}{p} \left( \frac{T_0}{T} \right)^{\delta - 1/2} \exp \left( - \frac{E_0}{k_0} \left( \frac{1}{T} - \frac{1}{T_0} \right) \right) \quad (6)$$

For given  $T$  and  $p$  this expression can be reformulated to allow for instance water vapor determination.

$$n_{H_2O} = \frac{k_\nu \cdot 1.132 \pi \alpha_0 p}{S_0 p_0} \cdot \left( \frac{T}{T_0} \right)^{\delta - 1/2} \exp \left( - \frac{E_0}{k_0} \left( \frac{1}{T} - \frac{1}{T_0} \right) \right) \quad (7)$$

A more thorough treatment of the DIAL technique should account for the Doppler and Voigt line shape too. However, since the subsequent error equations are also valid for the Doppler line shape and deviations from the Lorentz line shape in the troposphere are well within the errors of laser line shape knowledge, we omit in accordance with a statement by Megie et al (1983) a thorough treatment of Voigt line profiles.

### 3. ERROR ASSESSMENT

We define the error of a function  $f(x_i; i=1, \dots, m)$  by

$$\Delta f(x_i; i=1, \dots, m) = \sum_{i=1}^m \left| \frac{\partial f_i}{\partial x_i} \right| \Delta x_i \quad (8)$$

which resolved for  $\Delta x_j$  reads

$$\Delta x_j = (\Delta f - \sum_{i=1}^m \left| \frac{\partial f_i}{\partial x_i} \right| \Delta x_i) / \left| \frac{\partial f_i}{\partial x_j} \right| \quad (9)$$

ORIGINAL PAGE IS  
OF POOR QUALITY

Applying (9) to (3) we get for the absorption coefficient

$$\begin{aligned} \Delta k(r') &= \frac{1}{2(\Delta r)^2} \ln \left( \frac{P(r, \lambda_1) P(r-\Delta r, \lambda_2)}{P(r, \lambda_2) P(r-\Delta r, \lambda_1)} \right) \Delta r + 2 \left| \frac{1}{2\Delta r} \frac{1}{P(r', \lambda_1)} \right| \Delta P(r', \lambda_1) \\ &+ 2 \left| \frac{1}{2\Delta r} \frac{1}{P(r, \lambda_2)} \right| \Delta P(r, \lambda_2) \\ &\approx \frac{1}{\Delta r \cdot \text{SNR}_1} + \frac{1}{\Delta r \text{SNR}_2} \end{aligned} \quad (10)$$

The approximation uses  $P/\Delta P = \text{SNR}$  and neglects the first term in (10), which is of the order of  $10^{-6}$  to  $10^{-8}$  for an error of 10 m in the determination of  $\Delta r = 1$  km and for an optical depth  $\tau^* = k(r) \Delta r$  between  $10^{-3}$  and  $10^{-1}$ , while the second and the third vary from  $10^{-1}$  to  $10^{-3}$  for SNR between 1 and 100. Calculating  $\Delta T/T$  according to (9) using (6) yields

$$\frac{\Delta T}{T} = \frac{1}{\left| \frac{E_0}{k_0} \frac{1}{T} - \frac{1}{2} + \delta \right|} \left( \frac{\Delta P}{P} + \frac{\Delta n}{n} + \frac{1}{k_v} \cdot \left( \frac{1}{\Delta r \text{SNR}_1} + \frac{1}{\Delta r \text{SNR}_2} \right) \right) \quad (11)$$

The application of (9) to (7) finally gives the relative error  $n_{\text{H}_2\text{O}}/n_{\text{H}_2\text{O}}$  for water vapor profiling.

$$\frac{\Delta n}{n} = \frac{\Delta P}{P} + \left| \frac{E_0}{k_0} \frac{1}{T} + \frac{1}{2} - \delta \right| \frac{\Delta T}{T} + \frac{2}{\Delta r k_v \text{SNR}} \quad (12)$$

#### 4. THE SIGNAL-TO-NOISE RATIO

The error equations (10) - (12) mainly depend on SNR at the detector. The most important noise sources for this study (fixed to the  $.75 \mu\text{m}$  wavelength region) are:

- 1) shot noise caused by statistical fluctuations of photons constituting the signal current
- 2) background noise due to backscattered or reflected sun light

All other noise sources have been shown to be negligible (Endemann, 1983). For the above noise sources Megie and Menzies (1980) propose

$$\text{SNR} = \frac{N_k}{(N_k + N_B)^{1/2}} \quad (13)$$

with the number of backscattered photons received per unit time from layer k

$$N_k = \frac{P_k}{hf} \eta^* \frac{2\Delta r}{c} \quad (14)$$

and the number of background photons per unit time

$$N_B = \frac{I_B A^* \Omega^2 \pi B}{hf} \eta_1^* \eta_2^* \frac{2\Delta r}{c} \quad (15)$$

- $P_k$  = signal power from layer k after passage through the front filter in front of the detector
- $\eta_1^*$  = filter transmission
- $\eta_2^*$  = quantum efficiency of the detector
- $f$  = frequency ( $f = c/\lambda$ )
- $I_B$  = background radiance
- $\Omega$  = field of view of the receiver optics
- $B$  = filter bandwidth
- $h$  = Planck's constant

## 5. RESULTS

### 5.1 Impact of Variations in Aerosol Particle Concentration

Before we discuss the signal-to-noise ratio of the proposed system the errors due to random fluctuations of aerosol particle concentration in both the horizontal and vertical direction between two pulses of a multi-wavelength lidar are presented. Table 1 clearly demonstrates, that there is no way to get accurate profiles with only one laser shifting wavelength within 0.1 second. If particle concentration varies by only 0.1 percent - still unrealistically low - between two pulses, the relative error calculated from 100 trials with a random number generator reaches at the maximum 0.7, 0.4, and 2.1 percent for temperature T, pressure p and number density  $n_{H_2O}$  in the troposphere

Table 1: Maximum error in percent caused by variations in aerosol particle concentration between two pulses.

Variation	$\Delta T/T$	$\Delta p/p$	$\Delta n/n$ ( $H_2O$ )	level
1 %	20.0	8.0	37.0	troposphere
0.1%	1.6	2.3	11.0	stratosphere
	0.7	0.4	2.1	troposphere

### 5.2 Signal-to-Noise Ratio (SNR)

This section sticks to a two laser system, as shown to be necessary within the previous section. The separation of pulses has to be below a millisecond in order to neglect particle concentration changes. The SNR calculations include the major noise sources: shot noise and background noise of the sunlit atmosphere as expressed in (13) - (15). Other noise sources have been handled by Endemann (1983) and shown to be negligible for the proposed system whose performance will be tested under laboratory conditions.

SNR depends on such a variety of parameters that part of them has been fixed in order to assess the influence of some specifically. In accordance with the envisaged hardware development we have set:  $\eta_1^* = 0.45$ ,  $\eta_2^* = 0.18$  (Endemann, 1983a),  $A^* = 0.25 \text{ m}^2$ ,  $\Omega = 0.5 \text{ mrad}$ ,  $B = 1 \text{ nm}$ ,  $\Delta r = 1 \text{ km}$ ;  $I_B$  varies from 0 (night) to 5 (standard illumination) and  $200 \text{ W m}^{-2} \text{ sr}^{-1} \text{ m}^{-1}$  (strong sun glint or thick clouds). The central wavenumber  $\nu = 12975 \text{ cm}^{-1}$ ,  $P_0 = 25 \text{ MW}$ , and the height of the space craft varies from 250 to 800 km. The line parameters used are summarized in table 2. The first atmosphere adopted is a standard atmosphere for 60°N, July,

ORIGINAL PAGE 13  
OF POOR QUALITY

with 23 km horizontal visibility at the ground and an aerosol scale height of 1.25 km. The SNR values displayed in figures 1 and 2 for 250 and 800 km clearly demonstrate:

$SNR \approx 10$  for a single shot is only achievable within the troposphere. SNR for the on-line shot is drastically reduced for the stronger O<sub>2</sub> line. However, this does not mean enhanced temperature error, because the concomitant increase in optical depth  $\tau = \Delta r \cdot k(r')$  more than compensates this reduction. An additional constraint is: measurements must be taken outside sun glint areas. Within these first figures we did not tune aerosol backscattering in order to reach higher SNR.

Table 2: Lines and windows chosen

wavelength $\lambda$	wavenumber $\nu$	absorber and use	line strength $S_0$	halfwidth $\alpha_0$	lower state energy $E_0$
$\mu\text{m}$	$\text{cm}^{-1}$		cm	$\text{cm}^{-1}$	$\text{cm}^{-1}$
0.7707129	12975.000	window; T			
0.7711989	12966.823	O <sub>2</sub> ; T	0.734 10 <sup>-26</sup>	0.042	1803.18
0.7698983	12988.728	O <sub>2</sub> ; T	0.431 10 <sup>-25</sup>	0.042	1422.502
0.7866600	12711.972	H <sub>2</sub> O; n	0.362 10 <sup>-24</sup>	0.0655	704.214
0.7867201	12711.000	window; n			

<sup>+</sup> at 296 K and 1013.25 hPa

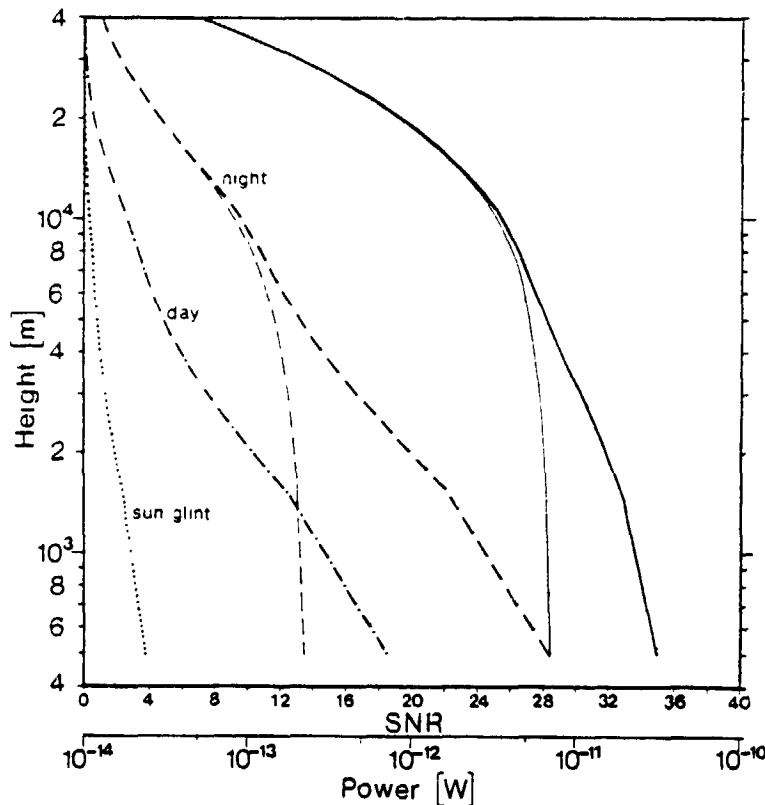


Figure 1: Vertical profiles of backscattered power (—) and SNR for a standard atmosphere at 60°N, July, with 23 km horizontal visibility, aerosol scale height 1.25 km, space craft at 250 km. The thicker curves stand for the weak O<sub>2</sub> line, thinner ones for the stronger line. Pulse energy for all the simulations is kept at 0.5 J.

ORIGINAL PAGE IS  
OF POOR QUALITY

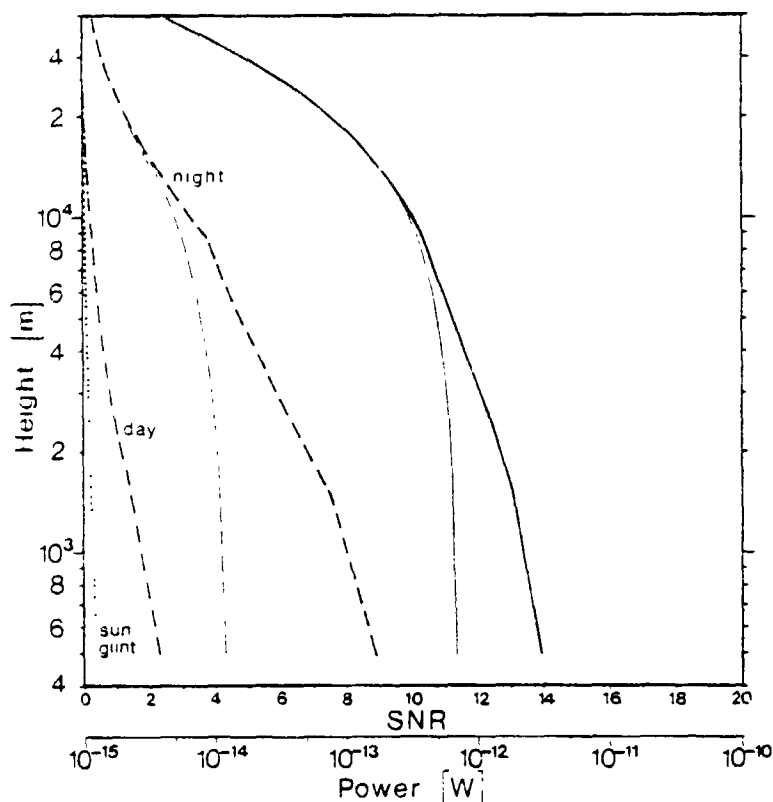


Figure 2: As fig.1, however space craft at 800 km

Since figures 1 and 2 show SNR for one pulse pair, an averaging over 100 pulse pairs, which will be tolerable from the point of view of horizontal resolution, gives  $SNR > 100$  in large parts of the troposphere for a space craft at 250 km. Using a standard aerosol model (Lenoble and Brogniez, 1983) for continental areas in the troposphere and a young (1 month) stratospheric aerosol layer of volcanic origin SNR is enhanced compared to the atmospheric model in figures 1 and 2, now surmounting the value 10 even for a space craft at 800 km under night conditions. All the other aerosol models proposed, which were input to our programme but are not shown, do not give strongly different results. They all point to the drastic dependence on aerosol particle concentration. Rayleigh scattering can not give high enough SNR.

### 5.3 Relative Temperature and Humidity Error

The error equations (11) and (12) were explored under a variety of situations. However, the only figure displayed already contains the main result. The temperature error  $\Delta T/T$  in the lowest troposphere (figure 4) for  $\Delta r=2$  km is below 2 K only for  $SNR_2$  (window wavelength)  $\geq 200$  and rather low total optical depth  $\tau^*$  of the line. For water vapor profiling very similar results exist. However, the relative error  $\Delta n/n$  at  $SNR_2 \geq 200$  is only below 0.1 at a  $E_0 = 900 \text{ cm}^{-1}$ . The dependence on  $\tau^*$  is unchanged.

ORIGINAL FILE #3  
OF POOR QUALITY

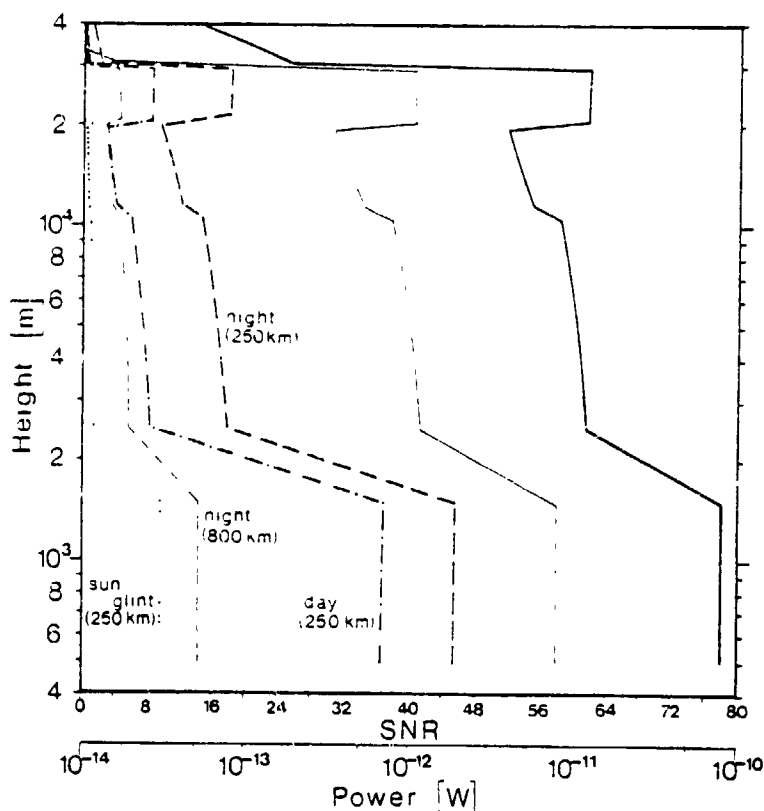


Figure 3: Vertical profiles of backscattered power (—) and SNR for a standard atmosphere at 60°N, July, with continental aerosol in the troposphere and volcanic aerosol in the stratosphere, one month after eruption. Thick lines for a space craft at 250 km, thin lines for a space craft at 800 km.

#### 6. ERRORS CAUSED BY THE FINITE WIDTH OF THE LASER LINE

Most simulations hitherto reported neglect the laser line width. According to Browell et al (1983) present lasers have a line width of 3 pm, corresponding to 0.05 cm<sup>-1</sup> at 0.7 μm. Korb and Weng (1982) assume 0.02 cm<sup>-1</sup>. Thus the laser line width is comparable to the halfwidth of the O<sub>2</sub> and H<sub>2</sub>O lines chosen. Since the above simulations assume the laser line to be monochromatic and to meet the absorption line center we have to assess the errors thus introduced. The optimal approach would be: revised analytic solutions. Here we adopt an inferior approach. We average transmissions due to gaseous absorption within one layer spectrally, symmetric to the line center. The differential absorption coefficients thus obtained are handled as before with the monochromatic approach. The result is a systematic error. Assuming a rectangular laser line of width 0.05 cm<sup>-1</sup> the relative temperature error varies from +1.1 percent in the upper atmosphere to -0.53 percent in the lower troposphere. Assuming a triangular distribution, where the laser line intensity has dropped to 1/8 at 0.025 cm<sup>-1</sup> distance from the center, ΔT/T lies between -0.01 and +0.12 percent. The relative humidity error Δn/n then varies between +2.0 and -0.95 percent.

ORIGINAL PAGE IS  
OF POOR QUALITY

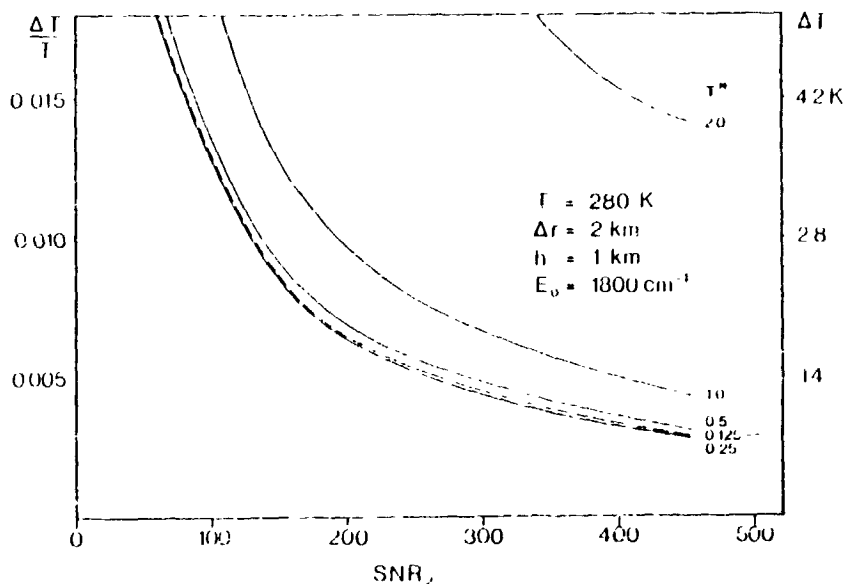


Figure 4: Relative temperature error  $\Delta T/T$  as a function of the signal-to-noise ratio for the window position,  $SNR_2$ , for different total optical depth  $\tau^*$  as indicated.

#### 7. FLUCTUATIONS OF LASER FREQUENCY

The instability of the laser frequency also causes errors, which in this case will not be systematic. After Browell et al (1983) contemporary lasers show fluctuations of  $\pm 0.3$  pm, approximately a tenth of the halfwidth of the absorption lines. We simulated these fluctuations by shifting the laser line in two different ways: 1) random shift with equal probability for all deviations within  $\pm 0.3$  pm; 2) random shift with a Gaussian distribution and a standard deviation  $\sigma = 0.3$  pm and accounting for a finite triangular laser line width of 3 pm (10% level).  $\Delta T/T$  varies from nearly 0 percent to 0.1 percent for both cases depending on height level. The values  $\Delta n/n$  reach 1.5 percent. This, however has to be compared to the  $\Delta n/n$  from (12) and thus is not intolerably high. All numbers reported are valid for the troposphere only and after an averaging over 100 realisations.

#### 8. INFLUENCE OF A POSSIBLE ABSORPTION LINE SHIFT WITH PRESSURE

The absorption lines of atmospheric gases are not fixed to a distinct wavelength. Their shift is negligibly small for many applications. The shift  $\delta = \alpha_0 / 2.75 p/p_0 (T_0/T)$  is comparable to the laser line shift.  $\delta$  ranges from  $0.002 \text{ cm}^{-1}$  at 50 hPa and 220 K to  $0.018 \text{ cm}^{-1}$  at the ground at 290 K. A laser signal thus centered at the absorption line at the tropopause is off the center to the shortwave wing of the line in the lower troposphere. The systematic error reaches -0.8 percent for  $\Delta T/T$  in the lower troposphere, while for the values  $\Delta n/n$  we have to expect up to -12 percent. There should again be pointed out, that the  $\delta$  chosen is a theoretical estimate which needs verification.

## 9. CONCLUSIONS

The major result of this study is:

Tropospheric temperature and humidity profiles in 1 to 2 km layers may be determined by a space borne DIAL using present technology to an accuracy of better than 2 K or 10 percent respectively under the following conditions:

- 1) Two laser system firing with a time lag below 1 millisecond.
- 2) Averaging over at least 100 pulses for a space craft at 250 km height.
- 3) Averaging over some hundred pulses for a space craft at 800 km.
- 4) Highest accuracy is found for both temperature and humidity with O<sub>2</sub> and H<sub>2</sub>O lines respectively at total optical depth at the line center within the 0.1 to 0.5 range.
- 5) The optical depth of the pure Rayleigh scattering atmosphere in window areas has to be strongly enlarged by aerosol particles, i.e. only turbid atmospheres give reliable results.

Major gaps found:

- 1) The impact of laser line width and laser line position fluctuations or accuracy has to be investigated in more detail.
- 2) The poor knowledge of absorption line shift with atmospheric pressure hampers an assessment of its importance for DIAL from space.

## 10. ACKNOWLEDGEMENT

The main part of this study has been funded by Battelle Institut, Frankfurt, FRG via a subcontract within a technology study of the European Space Agency.

## 11. REFERENCES

- Browell, E.V., Carter, A.F., Shipley, S.T., Allen, J.R., Butler, C.F., Mago, M.N., Siviter Jr, J.H., Hall, W.M. 1983: NASA Multipurpose Airborne DIAL System and Measurements of Ozone and Aerosol Profiles. Appl. Opt. 22, 522-534
- Endemann, M. 1983: Applications of Laser for Climatology and Atmospheric Research. Battelle Report for Contract No. 4868/81/NL/HP (SP)
- Endemann, M. 1983a: Private communication
- Korb, C.L. and Weng, C.Y. 1982: A Theoretical Study of a Two-Wavelength Lidar Technique for the Measurement of Atmospheric temperature Profiles. J. Appl. Met. 21, 1346-1355
- Lenoble, J. and Brogniez, C. 1983: A Comparative Review of Radiation Aerosol Models. Contr. Atm. Phys., in press
- Megie, G. and Menzies, R.T. 1980: Complementary of UV and IR Differential Absorption Lidar for Global Measurements of Atmospheric species. Appl. Opt. 19, 1173-1183
- Megie, G., Cahen, C. and Flamant, P. 1983: Comments on 'A Theoretical Study of a Two Wavelength Lidar Technique for the Measurement of Atmospheric Temperature Profiles. J. Climate a. Appl. Met. 22, 1136